Fabrication and characterization of multi-level hierarchical surfaces

Bharat Bhushan* and Hyungoo Lee

Received 23rd November 2011, Accepted 12th December 2011
DOI: 10.1039/c2fd00115b

A nanostructured surface may exhibit low adhesion or high adhesion depending upon fibrillar density, and it presents the possibility of realizing eco-friendly surface structures with desirable adhesion by mimicking the mechanics of fibrillar adhesive surfaces of biological systems. The current research uses a patterning technique to fabricate smart adhesion surfaces: one-, two- and three-level hierarchical synthetic adhesive structure surfaces with various fibrillar densities and diameters. The contact angles and contact angle hysteresis were measured to characterize the wettability. A conventional and a glass ball attached to an atomic force microscope (AFM) tip were used to obtain the adhesive forces *via* force–distance curves and to study the buckling behavior of a single fiber on the hierarchical structures.

1. Introduction

The mechanics of the fibrillar adhesive surfaces of biological systems such as a Lotus leaf and a gecko are widely studied due to their unique surface properties. The Lotus leaf is a model for superhydrophobic surfaces due to its extreme water-repellent properties, as well as self-cleaning properties and low adhesion. These properties are achieved by having a hydrophobic surface and a hierarchical structure with both micro- and nanoscale dimensions.[1–4] The contact angle depends on several factors, such as surface energy, surface roughness, and its cleanliness.[3,5–8] For hierarchical structures, the contact angle is dependent upon the heterogeneous (composite) interface present. For the heterogeneous interface, the contact angle is given by the Cassie–Baxter equation[9]

$$\cos\theta = R_f\cos\theta_0 - f_{LA}(R_f\cos\theta_0 + 1) \quad (1)$$

where θ is the contact angle on a rough surface, θ_0 is the contact angle on a smooth surface, f_{LA} is the fractional contact area of the liquid–air interface, and R_f is the surface roughness factor (>1) equal to the ratio of the real interface surface area (A_{SL}) to its geometric interface area (A_F), $R_f = A_{SL}/A_F$.

Geckos are well known for their exceptional ability to climb any wall and ceiling due to the micro/nano fibrillar hierarchical structure on their feet with about a billion fibers.[10–12] A nanostructured surface may exhibit low adhesion or high adhesion depending upon fibrillar density, and it presents the possibility of realizing eco-friendly surface structures with desirable adhesion. The adhesion mechanism of geckos is based on so-called division of contacts.[11,13] Cumulative van der Waals attraction results in strong adhesion. The adhesive force of a single contact, F_{ad}, based on the so-called Johnson–Kendall–Roberts (JKR) theory is given by[14]

Nanoprobe Laboratory for Bio- & Nanotechnology and Biomimetics, The Ohio State University, Columbus, OH, 43210, USA. E-mail: Bhushan.2@osu.edu

$$F_{ad} = \frac{3}{2}\pi W_{ad} R \tag{2}$$

where R is the radius of a spatula hemisphere tip, and W_{ad} is the work of adhesion (units of energy per unit area). It shows that the adhesive force of a single contact is proportional to the linear dimension of the contact. For a constant area divided into a large number of contacts or setae, n, the radius of a divided contact, R_1, is given by[13]

$$R_1 = \frac{R}{\sqrt{n}} \tag{3}$$

Therefore, the total adhesive force (F'_{ad}) for multiple contacts can be given by

$$F'_{ad} = \frac{3}{2}\pi W_{ad}\left(\frac{R}{\sqrt{n}}\right)n = \sqrt{n}F_{ad} \tag{4}$$

Thus, the total adhesive force increases linearly with the square root of the number of contacts. Based on this analysis, one needs to develop structures with a high density of nanofibers. A hierarchical structure is needed to provide adaptability to a variety of rough surfaces.[12]

In the present study, hierarchical-structured superhydrophobic surfaces have been fabricated using a porous membrane as a template. It is shown that one-, two-, and three-level fiber structures can be fabricated. Contact angle and AFM adhesion measurements were made. The buckling behavior of a single fiber on hierarchical structures was investigated.

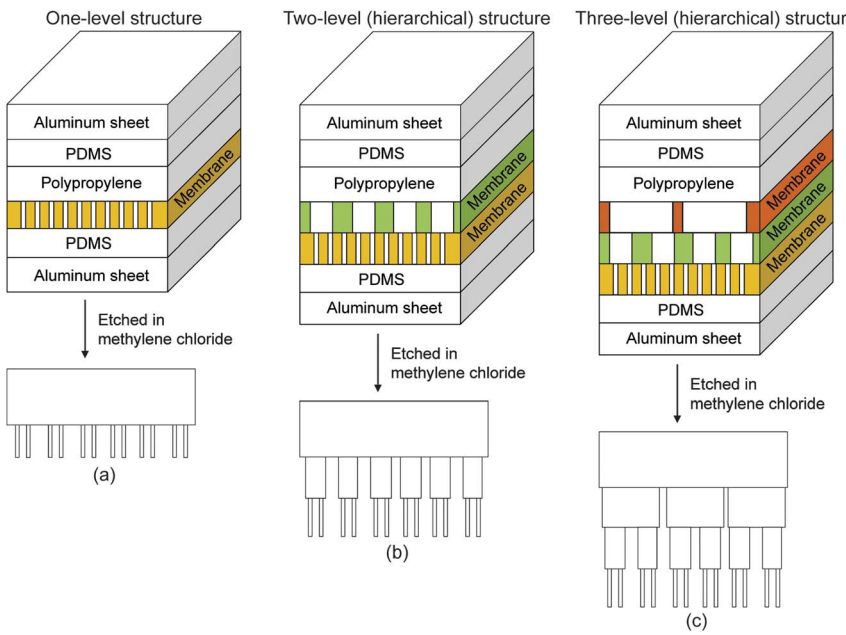

Fig. 1 Sample fabrication processes for (a) the one-level, (b) the two-level, and (c) the three-level fiber structures using one, two and three membranes in the stack, respectively. After heating the stacks in an oven, the membranes are etched using methylene chloride, to obtain the fibrillar samples.

2. Experimental

Polycarbonate (PC), a porous membrane with three pore sizes (600 nm, 5 μm, and 12 μm diameter), was used to create structures with different diameters and densities of fibers. All samples were fabricated using polypropylene (PP), a thermoplastic polymer. Fig. 1 shows the stacks used to fabricate one-, two-, or three-level structures. For the samples with a one-level structure (Fig. 1a), a PP film and a PC membrane were sandwiched between two polydimethylsiloxane (PDMS) disks, and the whole stack was again sandwiched between two aluminum sheets to provide support.[15,16] For fabricating the two- or three-level structures (Fig. 1b and 1c), a PP film was placed on two or three PC membranes with different sizes corresponding to two or three levels. The stacked layers were placed in an oven at 200 °C for 40–50 min with a weight of 1 kg in order to melt the PP and fill the pores in the membrane. The sandwiched samples were dipped into methylene chloride or a mixture of methyl chloride and chloroform for 1 h to etch the membranes to realize the polypropylene fibers. The controlled sample (flat surface) of PP was fabricated with no PC membrane by undergoing all steps used in processing the structured samples.

The wetting properties of the samples were characterized by contact angle measurement. The static contact angle (CA) was measured by placing a DI water droplet of about 5 μL on the samples using a microsyringe. Contact angle hysteresis (CAH) was also obtained by measuring the contact angle using a tilting stage with an automated goniometer (290-F4, Rame-Hart Instrument, Succasunna, NJ). The experiments were carried out at room temperature (21 °C) and in 45–55% relative humidity.

A commercial AFM (Nanoscope IIIa, Bruker, Santa Barbara, CA) was used for adhesion measurement and study of the buckling behavior of a single fiber. The AFM tip with 30 nm of nominal diameter (DNP, spring constant k of 3 N m^{-1}) was used to obtain the force–distance curves for each sample. To measure the adhesive force, a glass ball with a 30 μm diameter (dry soda lime glass microspheres, Duke Scientific, Palo Alto, CA) was attached to the AFM tip and used to obtain the force–distance curves.[3,12] The experiments were performed at room temperature (21 °C) and 45–55% relative humidity.

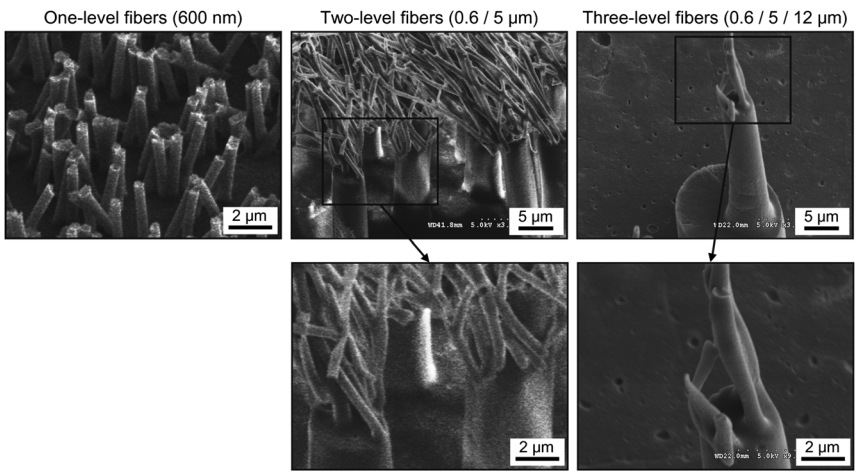

Fig. 2 SEM images of the samples. The one-level structure of 600 nm diameter fibers, the two-level structure of 600 nm diameter with 5 μm diameter fibers, and the three-level structure of 600 nm diameter with 5 μm diameter fibers on 12 μm diameter fibers, are shown.

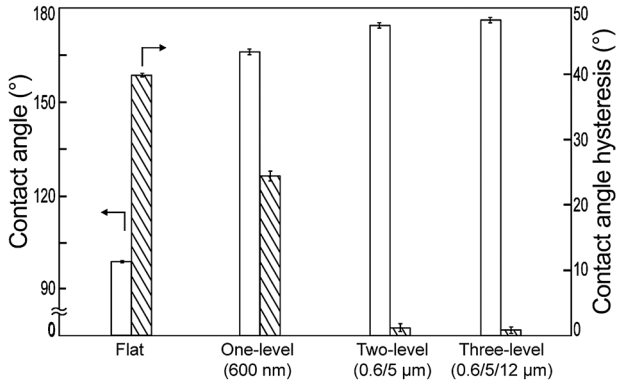

Fig. 3 The measured CAs and CAHs on the flat sample, and the one-, two-, and three-level fibers.

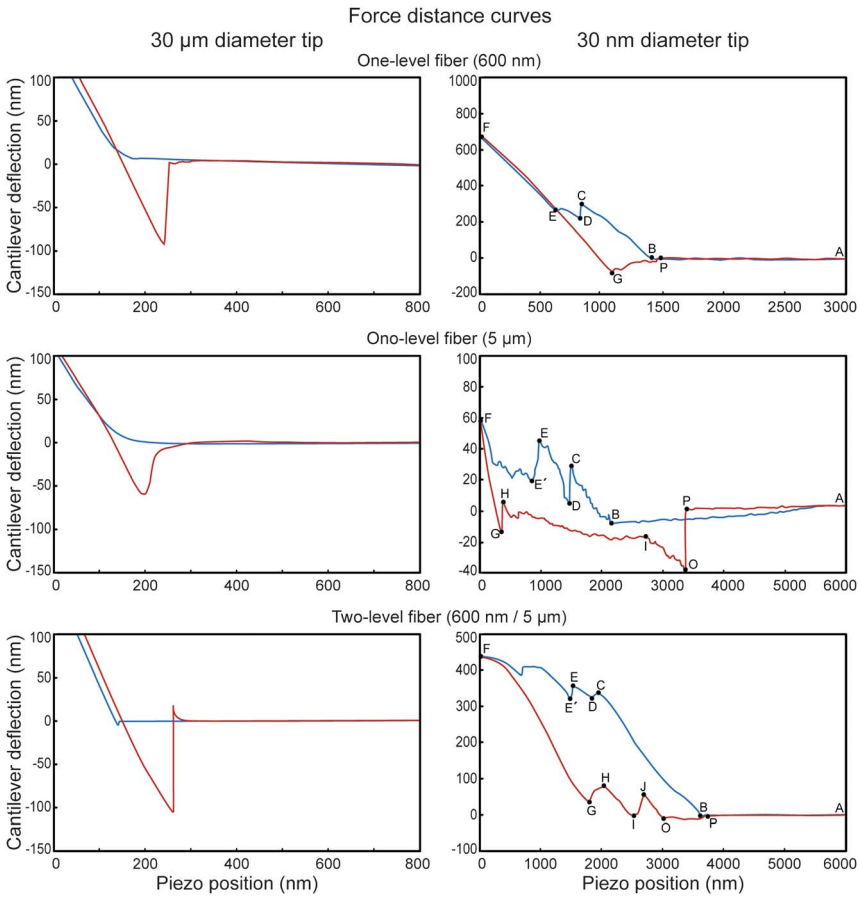

Fig. 4 Representative force–distance curves for the samples with the one-level (600 nm and 5 μm) and the two-level single fibers (600 nm/5 μm) obtained using the 30 μm diameter AFM tip (left column) and the 30 nm diameter AFM tip (right column).

3. Results and discussion

Using a polypropylene film and PC membranes with different pore sizes, the one-, two- and three-level fibrillar structures have been fabricated. The SEM images of the fabricated samples are shown in Fig. 2.

The wetting properties of the samples were characterized by the static contact angle (CA) and contact angle hysteresis (CAH) of a water droplet on each sample, as shown in Fig. 3. The CA (99°) of the flat (control sample) surface of PP indicates that PP is hydrophobic itself due to its low surface free energy (about 30 mJ m^{-2}). As the order of the fiber structure level increases, the CA increases due to the increase in surface roughness (R_f) and the formation of air-pockets (f_{LA}) under the water droplet. Increasing R_f and f_{LA} also leads to a decrease of the CAH.[1] The results show that the one-, two- and three-level fibrillar structures are superhydrophobic.

Adhesive forces (F_{ad}) of the one-level (600 nm and 5 μm) and two-level fibers were measured using the AFM tips. Representative force–distance curves are shown in Fig. 4. The left column is for data obtained using the 30 μm diameter tip, and the right column is for the 30 nm diameter tip. Bending or buckling behavior of the fibers was not observed in the force–distance curves in the left column.

In the right column in Fig. 4, bending and buckling behaviors of a one- and two-level fibers are shown while the 30 nm diameter tip travels downward. Fig. 5 shows the behavior of the two-level single fiber with the AFM tip. Schematics of the fiber behavior at each point as the AFM tip travels are also shown. The tip approaches the fiber (point A to B), and the tip touches the fiber at point B. From point B to C, the tip presses the fiber and is deflected so that the fiber is gradually bent and remains pressed. From point C to D, the fiber buckles. However, the tip keeps pressing the fiber from point D to E, inducing more compression of the fiber.

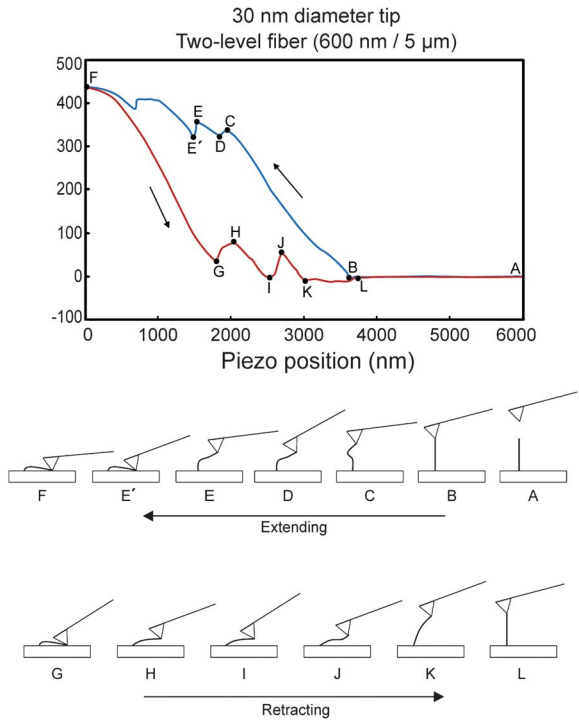

Fig. 5 The force–distance curve for the two-level single fiber (600 nm/5 μm) obtained using the AFM tip of 30 nm diameter. Schematics of the fiber behavior at each point as the AFM tip travels are shown.

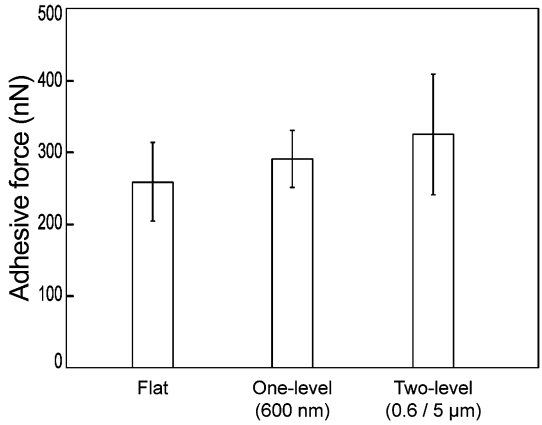

Fig. 6 Adhesive force of the flat sample, and the one- and two-level fiber samples measured using the 30 μm diameter tip. The measurements were performed at room temperature (21 °C) and 45–55% relative humidity.

From point E′ to F, even though the tip keeps pressing, the fiber is not bent or buckled any more so the tip is deflected. From point F, the tip retracts upward. Even though the tip retracts, the fiber does not stand back up (from point F to G). At point G, the fiber stands. From point H to I, the tip retracts, but the fiber does not move. From point I to J, the fiber stands up again. This phenomenon repeats at point K to L.

From the force–distance curves obtained using the 30 μm diameter tip (Fig. 4), the adhesive forces for the samples are calculated. The adhesive force values are plotted in Fig. 6. The force on the flat surface is 260 nN, but those on the one- and two-level fibers are 290 and 326 nN, respectively. This is attributed to the number of fibers. The flat surface can be considered as a fiber with a diameter larger than the real contact area between the AFM ball tip and the flat surface. As shown in eqn (4), with an increase in the number of fibers (n) the adhesive force increases in proportion to the square root of n. Moreover, it is expected that the AFM tip travels deeper into the fiber structures than for the flat sample as shown in the buckling experiment on the fibrillar structures (Fig. 5). It results in an additional increase of the adhesive force. The two-level fibrillar structures have an adhesive force slightly larger than the one-level structures. Although the density of the two-level fibrillar structures is lower than that of the one-level, the two-level structure is more compliant which leads to a larger number of fibers coming in contact with the tip, increasing the adhesive force.

4. Conclusions

In this study, a simple way to fabricate one-, two-, and three-level fiber structures has been developed. The wetting properties and the adhesive forces on the samples have been investigated. By measuring the CA and CAH of the samples, it is shown that the fiber structures exhibit superhydrophobicity. It is observed that the CA increases and CAH decreases with increasing R_f and f_{LA}.

The adhesive forces (F_{ad}) of the one- and two-level fibers are higher than that of the flat surface due to the increase of the number of fibers on the surfaces. It is shown that the more compliant the fiber structures are, the higher the adhesive forces are.

References

1 M. Nosonovsky and B. Bhushan, *Multiscale Dissipative Mechanisms and Hierarchical Surfaces: Friction, Superhydrophobicity, and Biomimetics*, Springer, Heidelberg, Germany, 2008.

2 *Springer Handbook of Nanotechnology*, ed. B. Bhushan, Springer, Heidelberg, Germany, 3rd edn, 2011.
3 *Nanotribology and Nanomechanics I – Measurement Techniques and Nanomechanics, II – Nanotribology, Biomimetics, and Industrial Applications*, ed. B. Bhushan, Springer-Verlag, Heidelberg, Germany, 3rd edn, 2011.
4 B. Bhushan and Y. C. Jung, *Prog. Mater. Sci.*, 2011, **56**, 1–108.
5 A. W. Adamson, *Physical Chemistry of Surfaces*, Wiley, NY, 1990.
6 J. N. Israelachvili, *Intermolecular and Surface Forces*, Academic, London, 2nd edn, 1992.
7 B. Bhushan, *Principles and Applications of Tribology*, Wiley, NY, 1999.
8 B. Bhushan, *Introduction to Tribology*, Wiley, NY, 2002.
9 A. B. D. Cassie and S. Baxter, *Trans. Faraday Soc.*, 1944, **40**, 546–541.
10 R. Ruibal and V. Ernst, *J. Morphol.*, 1965, **117**, 271–294.
11 K. Autumn, M. Sitti, Y. A. Liang, A. M. Peattie, W. R. Hansen, S. Sponberg, T. W. Kenny, R. Fearing, J. N. Israelachvili and R. J. Full, *Proc. Natl. Acad. Sci. U. S. A.*, 2002, **99**, 12252–12256.
12 B. Bhushan, *J. Adhes. Sci. Technol.*, 2007, **21**, 1213–1258.
13 E. Arzt, S. Gorb and R. Spolenak, *Proc. Natl. Acad. Sci. U. S. A.*, 2003, **100**, 10603–10606.
14 K. L. Johnson, K. Kendall and A. D. Roberts, *Proc. R. Soc. London, Ser. A*, 1971, **324**, 301–313.
15 M. Sitti, "High aspect ratio polymer micro/nano-structure manufacturing using nanoembossing, nanomolding and directed self-assembly", *Proc. IEEE/ASME Advanced Mechatronics Conference*, July 2003, pp. 886–890.
16 J. Lee, R. S. Fearing and K. Komvopoulos, *Appl. Phys. Lett.*, 2008, **93**, 191910.